Systems Pharmacology Modeling of Drug-induced Hyperbilirubinemia: Differentiating Hepatotoxicity and Inhibition of Enzymes/Transporters

K Yang[1], C Battista[1,2], JL Woodhead[1], SH Stahl[3], JT Mettetal[4], PB Watkins[2], SQ Siler[1] and BA Howell[1]

Elevations in serum bilirubin during drug treatment may indicate global liver dysfunction and a high risk of liver failure. However, drugs also can increase serum bilirubin in the absence of hepatic injury by inhibiting specific enzymes/transporters. We constructed a mechanistic model of bilirubin disposition based on known functional polymorphisms in bilirubin metabolism/transport. Using physiologically based pharmacokinetic (PBPK) model-predicted drug exposure and enzyme/transporter inhibition constants determined *in vitro*, our model correctly predicted indinavir-mediated hyperbilirubinemia in humans and rats. Nelfinavir was predicted not to cause hyperbilirubinemia, consistent with clinical observations. We next examined a new drug candidate that caused both elevations in serum bilirubin and biochemical evidence of liver injury in rats. Simulations suggest that bilirubin elevation primarily resulted from inhibition of transporters rather than global liver dysfunction. We conclude that mechanistic modeling of bilirubin can help elucidate underlying mechanisms of drug-induced hyperbilirubinemia, and thereby distinguish benign from clinically important elevations in serum bilirubin.

Study Highlights

WHAT IS THE CURRENT KNOWLEDGE ON THE TOPIC?
☑ Severe drug-induced liver injury increases serum bilirubin. However, drug-induced hyperbilirubinemia can also be induced by inhibition of enzymes/transporters that mediate bilirubin disposition.

WHAT QUESTION DID THIS STUDY ADDRESS?
☑ Can enzyme/transporter-mediated drug-induced hyperbilirubinemia be predicted by mechanistic modeling from *in vitro* inhibition data? Can a mechanistic model differentiate bilirubin increases due to overt liver injury vs. enzyme/transporter inhibition?

WHAT THIS STUDY ADDS TO OUR KNOWLEDGE
☑ The mechanistic bilirubin model, combined with PBPK model-predicted drug exposure and *in vitro* enzyme/transporter

inhibition constants, correctly predicted indinavir-mediated unconjugated hyperbilirubinemia and minimal bilirubin changes by nelfinavir. CKA induced ALT and bilirubin elevations in rats, and simulations suggest that CKA-mediated bilirubin elevation was mostly due to inhibition of bilirubin transporters, rather than liver injury.

HOW THIS MIGHT CHANGE CLINICAL PHARMACOLOGY OR TRANSLATIONAL SCIENCE
☑ Mechanistic modeling that represents hepatotoxicity mechanisms and enzyme-mediated and transporter-mediated bilirubin disposition can be used to elucidate underlying mechanisms of drug-induced hyperbilirubinemia and may be useful in prospective prediction of bilirubin increases by drug candidates.

Bilirubin, the product of heme breakdown from red blood cells, is exclusively eliminated by the liver. Thus, circulating bilirubin is widely used as a diagnostic biomarker for liver function. Large postmarketing studies of patients with drug-induced liver injury (DILI) show that ∼10% of subjects with hyperbilirubinemia or jaundice die or require a liver transplant.[1–3] In the setting of a clinical trial of a new drug candidate, elevations in serum bilirubin may also indicate severe liver injury with global hepatic dysfunction. The 2009 US Food and Drug Administration guidance

on assessing liver safety in clinical trials defines the "Hy's Law Case" as a trial subject who experiences a hepatocellular injury with concomitant elevations in serum alanine aminotransferase (ALT) >3× the upper limit of normal (ULN) and serum total bilirubin (TB) elevation >2× ULN when there is no more likely cause than the study drug. The existence of Hy's Law Cases in a clinical trial database is interpreted as indicating that the study drug is capable of causing liver failure, a conclusion that can lead to termination of the development program, requirement of

[1]DILIsym Services Inc., Research Triangle Park, North Carolina, USA; [2]University of North Carolina Institute for Drug Safety Sciences, The Eshelman School of Pharmacy, The University of North Carolina at Chapel Hill, Chapel Hill, North Carolina, USA; [3]ADME Transporters, Drug Safety and Metabolism, Innovative Medicines and Early Development, AstraZeneca, Cambridge, United Kingdom; [4]Drug Safety and Metabolism, AstraZeneca R&D, Waltham, Massachusetts, USA. Correspondence: K Yang (kyang@dilisym.com)
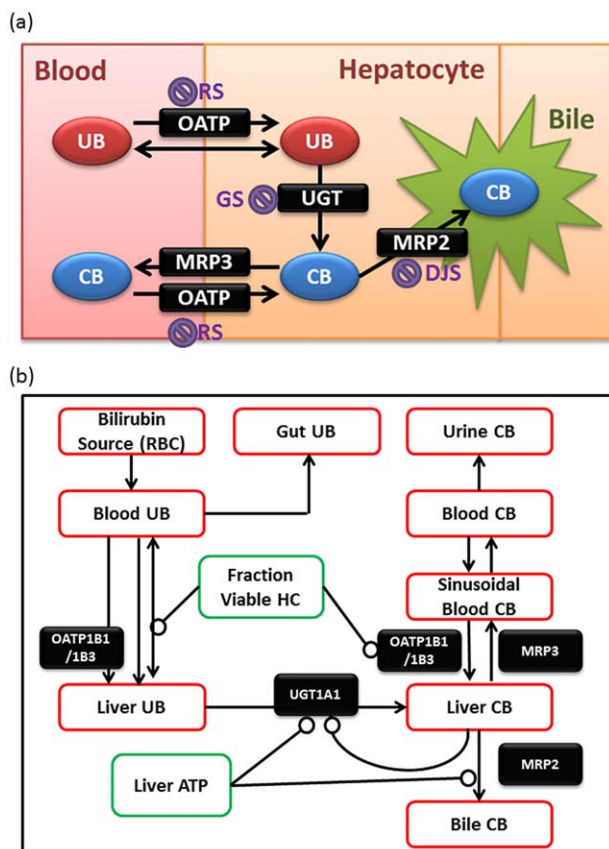
Figure 1 Diagrams of hepatobiliary disposition of bilirubin (**a**) and the bilirubin submodel structure within DILIsym (**b**). CB, conjugated bilirubin; DJS, Dubin-Johnson Syndrome; GS, Gilbert's Syndrome; HC, hepatocytes; MRP, multidrug resistance-associated protein; OATP, organic anion transporting polypeptide; RBC, red blood cell; RS, Rotor Syndrome; UB, unconjugated bilirubin; UGT, UDP glucuronosyltransferase.

extended clinical trials to assess risk management strategies, or restricted indications. Therefore, the observation of hyperbilirubinemia during clinical trials or postmarketing can raise concern about irreversible liver injury with serious regulatory consequences.

However, drug-induced hyperbilirubinemia is not always indicative of hepatotoxicity. Drugs may also increase serum bilirubin in the absence of hepatic injury by inhibiting enzymes/transporters that are involved in hepatic elimination of bilirubin. Serum bilirubin consists of conjugated bilirubin (CB) and unconjugated bilirubin (UB). UB is released to the circulation with red blood cell degradation and is taken up into hepatocytes by active transport (organic anion transporting polypeptide (OATP)1B1/1B3) and passive diffusion.[4–6] Once inside the hepatocytes, UB is metabolized to CB (glucuronide conjugate, primarily) by UDP glucuronosyltransferase (UGT)1A1.[7] Liver-generated CB is excreted into bile by multidrug resistance-associated protein (MRP)2, or transported back to sinusoidal blood by the efflux transporter MRP3, and then taken up again by downstream hepatocytes by OATP1B1/1B3.[6,8–10] Patients with inherited disorders of bilirubin metabolism and/or transport (e.g., Rotor Syndrome (RS), Gilbert's Syndrome (GS), Crigler-Najjar Syndrome (CNS), and Dubin-Johnson Syndrome (DJS)) exhibit elevated serum

bilirubin, suggesting that modulation of any of these enzyme-mediated and transport-mediated processes by drugs may increase serum bilirubin (**Figure 1**).[8,11–14] Several studies have reported that drugs with potent *in vitro* inhibition for enzyme/transporters that mediate bilirubin disposition at clinical exposure levels are associated with hyperbilirubinemia.[15–17]

Although the inhibitory potential for bilirubin enzyme/transporters can be assessed using *in vitro* studies, it remains a challenge to translate these *in vitro* data to *in vivo* and to predict the net effects of inhibition of multiple steps involved in bilirubin disposition. In addition, interpretation is not straightforward when hyperbilirubinemia is observed with and without concomitant serum ALT elevations in clinical trials. This is because some drugs without hepatic liabilities can cause high and frequent elevations in serum ALT.[1] In such cases, distinguishing hyperbilirubinemia that is mediated by liver injury from enzyme/transporter-mediated interaction is challenging.

Mechanistic modeling could provide a useful tool to investigate the underlying mechanisms of hyperbilirubinemia and/or predict this multifactorial event. DILIsym (the product of a public-private partnership involving scientists from industry, academia, and the US Food and Drug Administration) is a mechanistic, multiscale model of DILI that integrates pharmacokinetic and *in vitro* toxicity data to predict *in vivo* hepatotoxicity in humans and preclinical animals.[18] DILIsym can leverage existing preclinical and clinical data to predict the risk of hepatocellular DILI and prioritize drug candidates, and help optimize dosing paradigms and monitoring. Construction of SimPops, simulated populations that include variability in toxicity mechanisms, enabled prediction of low-frequency injuries as well as characterization of patients at DILI risk.[19,20] The current SimPops represent healthy subjects, and patients with diabetes or nonalcoholic fatty liver disease, but do not yet include ethnic differences or age-related changes nor represent variability in biomarker-related parameters. The bilirubin submodel within DILIsym was initially designed to predict hyperbilirubinemia due to severe liver injury.[21] In the current study, the bilirubin submodels for human and preclinical species were updated to represent enzyme/transporter-mediated bilirubin elimination. Serum bilirubin levels in patients and animals with impaired function of bilirubin enzyme or transporter(s) were used to determine the impact of each pathway on the changes in serum UB and CB. The impact of three compounds, indinavir, nelfinavir, and an investigational drug (chemokine receptor antagonist (CKA), 1-(4-chloro-3-(trifluoromethyl)benzyl)-5-hydroxy-1H-indole-2-carboxylic acid),[22] on bilirubin levels was simulated in humans and rats to validate the current model.

Indinavir and nelfinavir are protease inhibitors used to treat human immunodeficiency virus. Both drugs are known to inhibit UGT1A1 and OATP1B1,[15] but only indinavir is associated with hyperbilirubinemia.[23,24] Altered serum bilirubin levels by indinavir and nelfinavir were simulated with DILIsym by combining *in vitro* enzyme/transporter inhibition data with *in vivo* exposure predicted by physiologically based pharmacokinetic (PBPK) modeling. CKA was shown to inhibit multiple hepatic transporters.[22] CKA showed minimal to modest ALT increase in humans; whereas it induced dose-dependent serum ALT increases in rats.
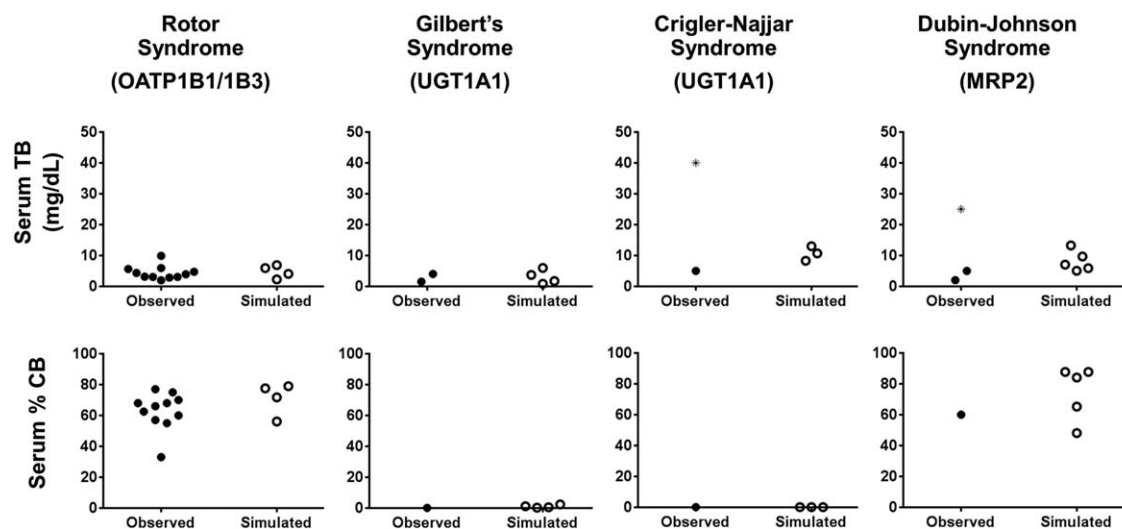
Figure 2 Simulated and observed bilirubin levels in patients with inherited disorders of bilirubin metabolism and transport. Top panels represent observed (closed circles)[8,11–14,27] and simulated (open circles) serum total bilirubin (TB) levels. Bottom panels represent observed (closed circles) and simulated (open circles) percent conjugated bilirubin (CB) in serum compared to serum TB. Multiple simulated individuals for each condition represent individuals with impaired enzyme/transporter function to a different extent within the ranges. Simulated patients have 70–95% impaired OATP1B1/1B3 function (Rotor Syndrome (RS)), 30–60% impaired UGT1A1 function (Gilbert's Syndrome (GS)), 70–90% impaired UGT1A1 function (Crigler-Najjar Syndrome (CNS)), or 50–90% impaired MRP2 function (Dubin-Johnson Syndrome (DJS)), respectively. Asterisks (*) represent less frequently observed serum TB ranges in patients with CNS or DJS.

Previous modeling with DILIsym using *in vivo* exposure and *in vitro* mechanistic toxicity data correctly predicted species differences in hepatotoxicity.[25] Interestingly, CKA induced hyperbilirubinemia in all the treated rats, whereas ALT elevations were observed only in a subset of treated rats, suggesting that factors other than liver injury might have contributed to the bilirubin increases. In the present study, CKA-mediated effects on serum bilirubin were simulated using *in vitro* bilirubin transporter inhibition data, PBPK-predicted exposure, and previously defined hepatotoxicity mechanistic parameters in simulated human and rat populations.

RESULTS

Simulation of bilirubin levels in patients with impaired bilirubin metabolism and transport

The normal range of serum TB is 0.1–1.2 mg/dL, and about 3.0–4.3% of serum TB exists as CB.[14] Respective baseline values in the current bilirubin model are 0.55 mg/dL and 3.6%. The bilirubin model parameters were optimized to clinical bilirubin data in patients with impaired bilirubin metabolism and transport (**Supplementary Table S2** online). RS is a genetic disorder characterized by near-complete loss of OATP1B1/1B3 expression.[8] Patients with RS present with conjugated hyperbilirubinemia, suggesting that (1) there exist non-OATP-mediated hepatic uptake pathway(s) for UB, and (2) OATP1B1/1B3 is involved in blood-hepatocyte shuttling of CB. Therefore, hepatic uptake of UB was represented by both non-OATP and OATP-mediated uptake processes, and hepatic uptake of CB was represented as an OATP1B1/1B3-mediated process. The serum TB and percent serum CB were 2.28–6.91 mg/dL and 56.1–79%, respectively, in the simulated patients with RS (with 70–95% impaired function

of OATP1B1/1B3), consistent with clinically observed values of 4.42 ± 2.18 mg/dL and 62.9 ± 12.1% (**Figure 2**).[8]

Patients with GS have ~30–50% of normal UGT1A1 function, whereas CNS is a rare genetic disorder with near-complete loss of UGT1A1 function. Patients with GS or CNS present with unconjugated hyperbilirubinemia; serum TB levels in patients with GS increase to 1.8–4 mg/dL, whereas patients with CNS manifest increased serum TB up to 6–44 mg/dL.[12,14] Simulated patients with GS and patients with CNS had impaired function of UGT1A1 by 30–60% and 70–90%, respectively. Simulated serum TB in respective groups were 0.84–5.99 and 8.32–13.03 mg/dL and were mostly composed of UB, consistent with the clinical data (**Figure 2**).

Patients with DJS, characterized by conjugated hyperbilirubinemia, have mutations in genes encoding MRP2. Patients with DJS have decreased MRP2 function and adaptive increases in MRP3 expression.[12] Thus, the simulated patients with DJS had impaired function of MRP2 by 50–90%, and MRP3 function increased threefold.[26] Patients with DJS manifest with conjugated hyperbilirubinemia; serum TB often increases up to 2–5 mg/dL, and, less often, up to 25 mg/dL.[27] Simulated serum TB levels in the patients with DJS were 5.08–13.28 mg/dL, 48–88% of which is conjugated, consistent with the clinical data (**Figure 2**).

Overall, simulations reasonably recapitulated conjugated hyperbilirubinemia in patients with RS or DJS, and unconjugated hyperbilirubinemia in patients with GS or CNS.

Simulation of bilirubin levels in rats and mice lacking enzyme or transporters

The normal range of serum TB and percent serum CB in rats and mice were highly variable (**Supplementary Table S1** online).
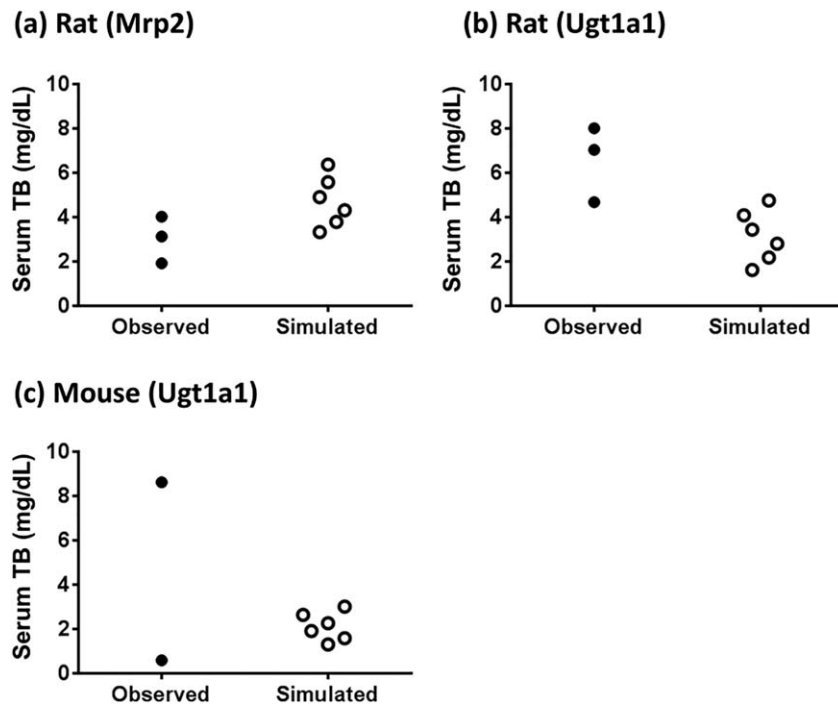
(a) Rat (Mrp2)

(b) Rat (Ugt1a1)

(c) Mouse (Ugt1a1)

Figure 3 Simulated and observed bilirubin levels in rats lacking Mrp2 or Ugt1a1, and mice lacking Ugt1a1. Closed and open circles represent observed and simulated serum total bilirubin (TB), respectively. (**a**) Observed data represent mean serum TB in Mrp2 knockout rats, EHBR rats, and TR⁻ rats (top to bottom).[41,46] Simulated rats have 50–100% impaired Mrp2 function. (**b**) Observed data represent mean serum TB in Ugt1a1 knockout rats obtained from multiple studies.[39,42,43,47] Simulated rats have 50–100% impaired Ugt1a1 function. (**c**) Observed data represent mean serum TB in Ugt1a1(-/-) (top) and Ugt1a1 (+/-) mice (bottom).[44] Simulated mice have 50–100% impaired Ugt1a1 function.

The baseline values of serum TB and percent serum CB in the current bilirubin model are 0.55 mg/dL and 3.6%, consistent with humans. The bilirubin model parameters were optimized to the bilirubin data in rats and mice lacking specific enzyme and/or transporter(s) that are involved in bilirubin disposition (**Supplementary Table S2** online). Simulations recapitulated conjugated hyperbilirubinemia in Mrp2-deficient (TR⁻), Eisai hyperbilirubinemic rat (EHBR), and Mrp2-knockout rats, which have impaired function of Mrp2 (observed and simulated serum TB: 1.9–4.0 vs. 3.3–6.4 mg/dL), unconjugated hyperbilirubinemia in Gunn rats with impaired function of Ugt1a1 (observed vs. simulated serum TB: 4.7–8.0 vs. 1.6–4.8 mg/dL), and Ugt1a1

knockout mice (observed vs. simulated serum TB: 7.8 ± 1.3 vs. 1.3–3.0 mg/dL; **Figure 3**).

The mouse bilirubin submodel recapitulated altered serum bilirubin levels in mice lacking single or multiple transporters; knockout of Mrp2 caused a modest increase in serum TB (observed vs. simulated changes from the baseline: 1.7-fold vs. 3.4-fold, respectively).[8] Knockout of Oatp1a/1b significantly increased serum TB (observed vs. simulated: 8.3-fold vs. 8.5-fold), which is reversed by additional knockout of Mrp3 (observed vs. simulated: 3.1-fold vs. 2.6-fold), but potentiated by additional knockout of Mrp2 (observed vs. simulated: 21.9-fold vs. 12.5-fold; **Figure 4**). Due to large variability in the mouse data, fold-
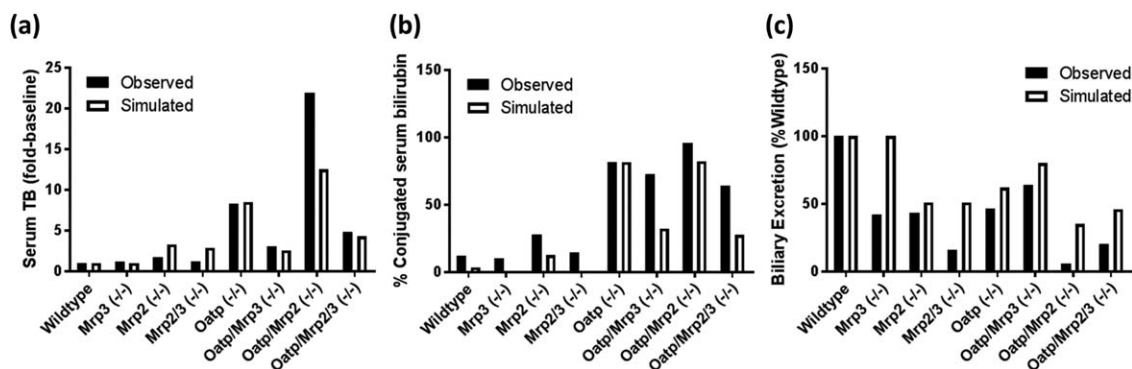

Figure 4 Simulated and observed bilirubin levels in mice lacking single or multiple transporters. Observed (closed bars)[8] and simulated (open bars) serum total bilirubin (TB) (**a**), percent conjugated bilirubin (CB) in serum compared to serum TB (**b**), and biliary excretion of TB presented as percent of wild-type animals (**c**).
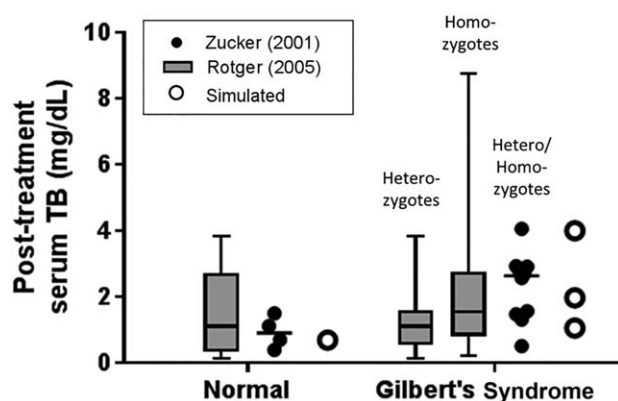
Figure 5 Indinavir-mediated hyperbilirubinemia in normal patients and patients with Gilbert's syndrome (GS) administered 800 mg indinavir t.i.d. for 1 month. For the data reported by Rotger et al.,[24] boxes represent 25th–75th percentile of the observed data, and whiskers represent the minimum and maximum observed data; serum total bilirubin (TB) levels in individuals with heterozygote and homozygote for GS alleles are presented separately. Zucker et al.[23] reported individual TB levels, which are represented with closed circles; the whisker represents the median value. Simulated normal individuals have unimpaired UGT1A1 function, whereas simulated patients with GS have 40–60% impaired UGT1A1 function.

change from the baseline was used for model optimization and validation to data.

Simulation of indinavir-mediated hyperbilirubinemia

Indinavir is predominantly eliminated by CYP3A4-mediated metabolism. Nonlinear pharmacokinetic profiles were observed at therapeutic doses (400–800 mg) due to saturation of hepatic CYP3A4.[28] Incorporation of saturable metabolism reasonably captured observed nonlinear pharmacokinetics in humans and rats; peak plasma concentration (C_{max}) and area under the curve (AUC) were within 1.5-fold of those from the mean observed plasma concentrations in humans and rats (**Supplementary Figure S1** online).

Simulations reasonably predicted increases in serum bilirubin (mostly UB) in normal patients after administration of indinavir. After administration of 800 mg indinavir t.i.d. for 1 month, simulations predicted unconjugated hyperbilirubinemia (pretreatment and post-treatment serum TB: 0.55 and 0.70 mg/dL, respectively), which is consistent with reported clinical data (pretreatment and post-treatment serum TB: 0.5 ± 0.28 and 0.84 ± 0.36 mg/dL, respectively; **Figure 5**).[23] Simulations also predicted that indinavir-induced hyperbilirubinemia is more pronounced in individuals possessing GS alleles, consistent with the clinical data; simulated serum TB in patients with GS administered 800 mg indinavir t.i.d. for 1 month was 2.34 ± 1.51 mg/dL, whereas the observed value combined from multiple studies was 2.06 ± 1.79 mg/dL (**Figure 5**).[23,24]

After oral administration of four doses of 240 mg/kg indinavir every 8 h, simulations predicted unconjugated hyperbilirubinemia (pretreatment and post-treatment serum TB: 0.55 and 0.80 mg/dL; 1.45-fold increase). Simulated fold-change in serum TB was consistent with reported preclinical data (pretreatment and post-treatment serum TB: 0.050 ± 0.002 and 0.070 ± 0.003 mg/dL, respectively; 1.4-fold increase).

Simulation of nelfinavir effects on serum bilirubin

Simulated nelfinavir serum profiles reasonably described the observed data in humans (**Supplementary Figure S1** online). Simulated plasma C_{max} and AUC were within 1.4-fold of those from the mean observed plasma concentrations in humans.[29,30] Nelfinavir was shown to inhibit UGT1A1 and OATP1B1 in in vitro assays, but is not associated with drug-induced hyperbilirubinemia (**Table 1**). Simulation of clinical dosing of nelfinavir (1,250 mg b.i.d. for 1 month) did not increase serum TB, consistent with clinical data.

Species differences in chemokine receptor antagonist-mediated hyperbilirubinemia

In the human SimPops administered single doses of up to 900 mg CKA, serum bilirubin did not exceed the ULN for any simulated individual, consistent with the clinical data. Conversely, the rat SimPops predicted dose-dependent serum bilirubin elevations at 50–500 mg/kg doses, consistent with preclinical data, although the magnitude of increase was underestimated (**Figure 6a**). In the preclinical studies, the mean fold-increase in serum TB was 2.1, 3.9, and 5.6 at 50, 200, and 500 mg/kg doses, respectively. Simulations predicted average serum TB increase of 1.4, 1.7, and 2.1-fold at respective doses (**Figure 6a**). When the same dosing protocols were simulated without considering inhibition of bilirubin transporters, serum TB levels minimally changed; predicted fold-increase in serum TB was 1.0, 1.1, and 1.2 at respective doses (**Figure 6b**). On the other hand, simulations with only bilirubin transporter-inhibition constants predicted 1.4-fold, 1.7-fold, and 1.9-fold increase in serum TB at

Table 1 Summary of inhibition constants of indinavir, nelfinavir, and chemokine receptor antagonist for enzymes and transporters involved in bilirubin disposition

Enzyme/transporter	Indinavir	Nelfinavir	CKA
OATP1B1 IC$_{50}$ (µM)	4.1 ± 1.8[a]	2 ± 0.9[a]	0.90[b]
OATP1B3 IC$_{50}$ (µM)	>100[a]	>100[a]	N/A
UGT1A1 IC$_{50}$ (µM)	6.8 ± 1.0[c]	4.8 ± 0.1[c]	N/A
MRP2 IC$_{50}$ (µM)	>100[d]	>100[d]	68.5 ± 7.3[e]
MRP3 IC$_{50}$ (µM)	N/A	N/A	11.2[f]

CKA, chemokine receptor antagonist, N/A, not available.
[a]Determined from HEK cells transfected with OATP1B1 or OATP1B3 using pitavastatin as a probe substrate.[15] [b]The average of IC$_{50}$ values from two independent studies (0.84 and 0.97 µM, respectively), each performed in triplicate. Inhibition of OATP1B1 activity was determined in a stably transfected HEK293 cell line that overexpressed the transporter using the probe substrate estradiol 17β-glucuronide (EG). CKA at varying concentrations was pre-incubated for 15 min at 37°C, followed by a 2-min incubation in presence of CKA and 5 µM EG at 37°C. EG was quantified via liquid chromatography mass spectrometry. [c]Determined from the human liver microsome using β-estradiol as a probe substrate.[15] [d]Determined using MRP2 PREDIVEZ kit (Solvo) and (5(6)-carboxy-2′,7′-dichlorofluorescein (CDF)) as a probe substrate.[15] [e]Data represent geometric mean and SD of four separate test occasions, each performed in duplicate. Effects of CKA on Mrp2 activity were determined by quantifying inhibition of ATP-dependent uptake (5 min, 37°C) of 10 µM CDF into inverted plasma membrane vesicles prepared from Sf21 insect cells expressing Mrp2. CDF was quantified via fluorescence.[22] [f]Determined from one independent study performed in triplicate. Inhibition of MRP3 activity was determined from inverted membrane vesicles prepared from HEP293 cells expression MRP3 using EG as a probe substrate.
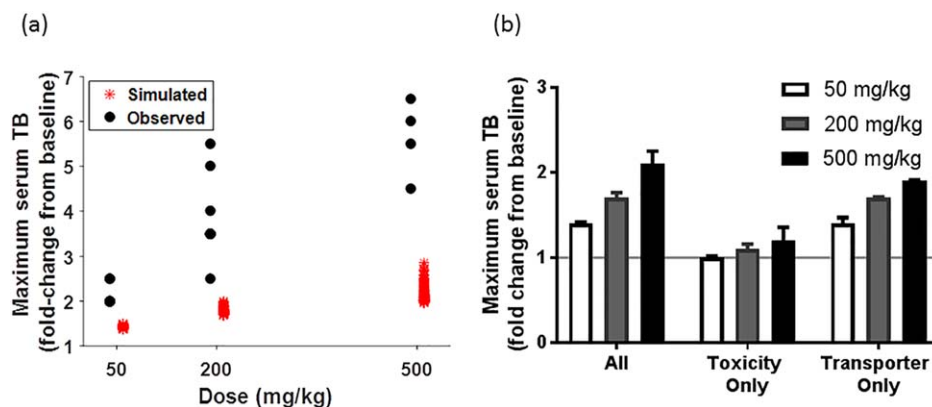
Figure 6 Simulated and observed peak serum total bilirubin (TB) levels in rats administered 50, 200, or 500 mg/kg chemokine receptor antagonist (CKA). (**a**) Maximum serum TB fold-change from baseline for increasing doses of CKA. Black dots represent data from preclinical trials and red asterisks denote simulation results for SimPops ($n = 294$) with combined effects of hepatotoxicity and bilirubin transporter inhibition. (**b**) Maximum serum TB fold-change from baseline for increasing doses of CKA simulated with combined effects of hepatotoxicity and bilirubin transporter inhibition, hepatotoxicity only, or bilirubin transporter inhibition only.

respective doses, indicating that bilirubin transporter inhibition was the main contributor to the simulated serum TB increase.

DISCUSSION

Drug-induced hyperbilirubinemia may occur because of severe DILI. The bilirubin submodel within DILIsym, which was initially designed to predict impaired liver function, reasonably recapitulated hyperbilirubinemia induced by hepatotoxic compounds, such as troglitazone.[20] However, drugs may increase serum bilirubin by inhibition of enzymes and/or transporters involved in bilirubin disposition in the absence of overt liver injury. In the current study, the bilirubin submodels for human and preclinical species were updated to represent enzyme-mediated and transporter-mediated bilirubin disposition; simulated quantitative effects of impaired function of enzymes/transporters on serum bilirubin levels were optimized using *in vivo* bilirubin data from humans and animals with impaired bilirubin metabolism and transport. Next, the impact of multiple enzyme/transporter inhibitors, indinavir, nelfinavir, and CKA, on serum bilirubin was simulated by combining PBPK-predicted drug disposition, the bilirubin model constructed in this study, and inhibition constants for enzyme and/or transporters measured *in vitro*. CKA simulations also incorporated known hepatotoxicity mechanisms to simulate net effects of liver injury and inhibition of bilirubin disposition. For each compound, simulated bilirubin levels were compared to *in vivo* preclinical/clinical bilirubin data to assess the predictive performance of the current bilirubin model.

Depending on the main bilirubin species in serum, hyperbilirubinemia is classified as unconjugated or conjugated hyperbilirubinemia. Two main reasons for unconjugated hyperbilirubinemia are increased bilirubin production (e.g., hemolytic anemias, hemolysis) and defective hepatic bilirubin metabolism. The current bilirubin submodel reasonably recapitulated unconjugated hyperbilirubinemia in patients with GS and CNS, Gunn rats, and Ugt1a1 knockout mice (**Figures 2 and 3**). Conjugated hyperbilirubinemia can result from defective hepatobiliary transport of CB, such as cholestatic defects, biliary obstruction, and

genetic disease, including DJS and RS. Patients with RS present near complete loss of OATP1B1/1B3 function. At first glance, it seems counterintuitive that impaired function of the uptake transporter increases serum CB because CB is generated in the liver and mostly excreted into bile via MRP2. The study by van de Steeg et al.[8] suggested that although most of the CB is eventually excreted into bile, CB may undergo liver-blood circulation to transfer CB from upstream hepatocytes to downstream hepatocytes. In the recirculation process, MRP3 mediates the efflux of CB from hepatocytes to sinusoidal blood, and OATP1B1/1B3 mediates reuptake of CB into the downstream hepatocytes. As a result, inhibition of OATP1B1/1B3 prevents reuptake of CB, leading to conjugated hyperbilirubinemia. By representing the cycling of CB between liver and sinusoidal blood, conjugated hyperbilirubinemia in patients with DJS and RS were reasonably reproduced with the current bilirubin submodel (**Figure 2**). Interestingly, a search for endogenous markers for OATP1B1/1B3-mediated drug-drug interaction reported that serum UB and CB are sensitive markers for OAPT1B1/1B3 inhibition by rifampin.[31] Altogether, these data support the role of OATP1B1/1B3 in hepatic uptake of both UB and CB.

Indinavir and nelfinavir inhibit UGT1A1 and OATP1B1, but only indinavir has been associated with hyperbilirubinemia. Simulations reasonably predicted indinavir-mediated unconjugated hyperbilirubinemia in normal patients, which was more pronounced in individuals possessing GS alleles, consistent with the clinical data.[23,24] Rotger et al.[24] reported a similar extent of increase in median bilirubin levels between normal subjects and patients with GS treated with atazanavir or indinavir (0.75 vs. 0.7–1.0 mg/dL), suggesting that higher bilirubin increases in patients with GS result from additive effects of impaired UGT1A1 function and indinavir-mediated UGT1A1/OATP1B1 inhibition. On the other hand, Zucker et al.[23] reported greater bilirubin increases in patients with GS compared with normal subjects after indinavir treatment (1.36 ± 1.05 vs. 0.39 ± 0.3 mg/dL), suggesting synergistic effects. Simulations predict slightly greater bilirubin increase in patients with GS

compared with normal subjects (0.21–0.30 vs. 0.14 mg/dL), which is more consistent with the Rotger *et al.*[24] data. Underlying reasons for the seemingly synergistic increase in patients with GS reported by Zucker *et al.*[23] still remain to be investigated. The current model also correctly predicted the minimal impact of nelfinavir on serum bilirubin. Although the inhibition potency and systemic exposure were comparable, nelfinavir showed higher protein binding (fraction unbound in plasma: 0.001 vs. 0.36), which led to lower unbound concentrations in the liver and sinusoidal blood, which mainly contributed to differential effects on serum bilirubin.[15]

CKA induced dose-dependent serum ALT and bilirubin elevations in rats, whereas only modest increases in ALT and no bilirubin increases were observed in humans. *In vitro* assays showed that CKA inhibited multiple bile acid and bilirubin transporters, inhibited mitochondrial electron transport chain (ETC) function, and induced oxidative stress.[22,25] Our previous modeling using DILIsym correctly predicted minimal ALT elevations in humans up to 900 mg, and dose-dependent, reversible ALT elevations in rats administered single oral doses of 50–500 mg/kg CKA.[25] CKA modeling with its hepatotoxic mechanistic data combined with bilirubin transporter inhibition correctly predicted minimal bilirubin increases in humans up to 900 mg, and dose-dependent bilirubin increases in rats at 50–500 mg/kg, although fold-changes were underestimated. To determine the underlying mechanism of bilirubin increase in rats, simulations were performed either only with hepatotoxic mechanistic inputs or only with bilirubin transporter inhibition. Simulation results indicate that, although ALT and bilirubin were concomitantly increased, bilirubin increases were mostly due to OATP1B1 and MRP2 inhibition, with minor contributions from liver injury. A previous study[22] showed no histological features indicative of overt hepatotoxicity in rats administered up to 500 mg/kg CKA, supporting the conclusion of the current study. Reasonable prediction of serum ALT, a biomarker of liver injury, also validates the quantitative contribution of liver injury assessed by the current model.[25]

Differences between observed and simulated fold-change bilirubin levels in rats administered CKA are likely due to multiple reasons. The main reason is a lack of metabolite effects in the simulations. CKA glucuronide was also shown to be a potent inhibitor of MRP2, but disposition of CKA glucuronide was not represented in the PBPK framework due to a lack of available pharmacokinetic data. If the metabolite had been included, it is very likely that bilirubin levels would have further increased in the simulations. Another reason could be lack of variability in parameters surrounding the bilirubin model. As currently modeled, all individuals in the SimPops have the same initial bilirubin parameter values and variability in bilirubin metabolism and transport processes were not represented, which leads to minimal bilirubin variability in the simulation results. By design, SimPops were constructed to represent variability in a large number of parameters related to toxicity mechanisms. If parameters related to biomarkers (e.g., bilirubin disposition) are also varied, it would require much larger populations (thousands instead of hundreds)

to cover all the parameter spaces, which would significantly increase computation time.

Not representing metabolite effects and interindividual variability in bilirubin disposition are limitations of the current study. Assessment of metabolite effects on hepatotoxicity and enzyme/transporter function could provide reliable predictions, but identification and synthesis of stable metabolites are not feasible especially during early stages of drug development. Also, future efforts will be needed to incorporate variability in baseline bilirubin levels, variability in multiple bilirubin disposition pathways, as well as environmental effects, such as caloric intake,[32,33] which may potentially impact serum bilirubin levels. Accurate prediction of the drug concentration in the liver is important in predicting inhibition of hepatic enzyme/transporters, but clinical measurement of liver concentration is challenging and there exists uncertainty in PBPK-predicted liver concentrations of the hepatic uptake transporter substrates based on the plasma profile.[34] In the current study, nelfinavir liver concentrations were predicted using a PBPK model trained to the plasma concentrations, which is another limitation. To explore the potential impact of the uncertainly in liver concentration, simulations were performed with up to 10-fold increases in nelfinavir liver concentrations. Nelfinavir still did not induce hyperbilirubinemia, supporting our overall conclusion.

Drugs may induce hyperbilirubinemia due to liver injury, inhibition of bilirubin enzymes and transporters, or a combination of both. Observations of drug-induced hyperbilirubinemia in clinical trials often require thorough assessments of hepatotoxic potential and investigation of underlying mechanisms. This would involve measurement of *in vivo* liver safety biomarkers and mechanistic *in vitro* studies. Given the complexity of underlying mechanisms and multifactorial nature of drug-induced hyperbilirubinemia, interpretation and translation of various data is not always straightforward. In the current study, a quantitative systems pharmacology model that incorporates drug disposition, the hepatocyte life cycle, multiple hepatotoxic mechanisms, and mechanistic biomarker models was used to assess underlying mechanisms of drug-induced hyperbilirubinemia. Differential effects of indinavir and nelfinavir on serum bilirubin were correctly predicted, and species differences in CKA-mediated hyperbilirubinemia were reasonably reproduced. Simulations also suggested that bilirubin increases in rats administered CKA were mainly due to bilirubin transporter inhibition with some contribution of liver injury, demonstrating that the current approach may be useful in predicting potential hyperbilirubinemia and assess underlying mechanisms for observed bilirubin increase *in vivo*.

METHODS
DILIsym bilirubin submodel update
Representation of bilirubin disposition in DILIsym prior to version 5A was published elsewhere and also described in the **Supplementary Methods** online.[21] In the current study, the bilirubin submodel was updated explicitly to represent the enzyme-mediated and transporter-mediated hepatobiliary disposition of bilirubin. In the bilirubin submodel, both serum and liver bilirubin pools consist of UB and CB. OATP1B1/1B3 facilitates hepatic uptake of UB and CB.[4–6] UB can also enter the liver

by passive diffusion.[35,36] Conversion of UB to CB in the liver is mediated by UGT1A1.[7] CB is excreted into bile via MRP2 or transported to sinusoidal blood by MRP3.[9] Each of the enzyme-mediated or transporter-mediated processes can be competitively inhibited by drugs or metabolites. Inhibition of OATP1B1/1B3 is dependent on the unbound drug concentration in hepatic inlet, which is the weighted average (by blood flow rate) of the portal vein concentration and the hepatic artery concentrations. Inhibition of UGT1A1, MRP2, and MRP3 is dependent on the unbound drug concentration in the liver. Renal excretion and intestinal secretion pathways are added as compensatory excretion pathways for CB and UB, respectively, under hyperbilirubinemia.[37–40]

The human bilirubin submodel was calibrated using bilirubin levels in humans with inherited disorders of bilirubin metabolism (i.e., GS and CNS) and transport (RS and DJS).[8,11–14,27] Bilirubin submodels for the rat, mouse, and dog were calibrated using bilirubin levels in preclinical species lacking specific enzymes or transporters (i.e., TR⁻, EHBR, Mrp2-knockout, and Gunn rats; mice lacking Mrp2, Mrp3, Oatp, or Ugt1a1; and dogs with biliary obstruction).[8,39,41–47] Affinities of UB and CB for enzymes and transporters were obtained from literature or optimized, if unavailable.[4,5,9,48] Parameters in the bilirubin submodel, obtained from the literature or estimated using serum bilirubin levels, are listed in **Supplementary Table S2** online. Detailed methods for bilirubin submodel construction can be found in the **Supplementary Method** online.

Development of physiologically based pharmacokinetic models

PBPK models were developed in DILIsym to describe the disposition of indinavir, nelfinavir, and CKA in humans and rats. Briefly, the PBPK model consisted of a central compartment representing the blood, three liver compartments representing three zones of the liver, and extrahepatic tissues (i.e., muscle, gut, and other tissues). Blood and tissue compartments were linked by blood flow. Tissue distribution of indinavir, nelfinavir, and CKA was represented with tissue partition coefficients; hepatic distribution of nelfinavir was transporter-mediated. Indinavir and nelfinavir are mainly eliminated by hepatic metabolism, which is represented by Michaelis-Menten kinetics. Metabolite disposition was not tracked because metabolite effects on bilirubin disposition remain unknown. Thus, it was assumed that only the parent modulated bilirubin disposition. Drug-specific parameters, obtained from the literature or estimated using available plasma and/or liver PK profiles of indinavir and nelfinavir, are listed in **Supplementary Table S3** online. PBPK parameters for CKA were previously reported.[25] Physiological parameters for tissue volumes and blood flows in the PBPK submodel of DILIsym were published elsewhere.[49]

Simulation of drug-induced hyperbilirubinemia

Indinavir-mediated hyperbilirubinemia was simulated in the baseline human and the baseline rat using PBPK model-predicted exposure and *in vitro* inhibition constants for UGT1A1, OATP1B1, and MRP2 (**Table 1**). In human simulations, the baseline human and a simulated patient with GS, which possess decreased UTG1A1 function by 40–60%, were orally administered 800 mg indinavir three times per day for 1 month. In rat simulations, the baseline rat was administered a total of four oral doses of 240 mg/kg indinavir every 8 h. Nelfinavir-mediated hyperbilirubinemia was simulated in the baseline human administered 1,250 mg nelfinavir b.i.d. for 1 month using PBPK model-predicted exposure and *in vitro* inhibition constants for UGT1A1, OATP1B1, and MRP2 (**Table 1**). CKA-mediated hyperbilirubinemia was simulated in the human (600 and 900 mg single oral dose) and rat (50, 200, and 500 mg/kg single oral dose) SimPops using PBPK model-predicted exposure, *in vitro* inhibition constants for OATP1B1 and MRP2 (**Table 1**), and previously determined *in vitro* mechanistic toxicity data.[25]

Additional Supporting Information may be found in the online version of this article.

AUTHOR CONTRIBUTIONS
K.Y., C.B., J.L.W., S.H.S., J.T.M., P.B.W., S.Q.S., and B.A.H. wrote the manuscript. K.Y., C.B., J.L.W., S.H.S., J.T.M., P.B.W., S.Q.S., and B.A.H. designed the research. K.Y., C.B., J.L.W., S.H.S., and J.T.M. performed the research. K.Y., C.B., J.L.W., S.H.S., J.T.M., P.B.W., S.Q.S., and B.A.H. analyzed the data.

1. U.S. Food and Drug Administration Guidance for Industry Drug-Induced Liver Injury: Premarketing Clinical Evaluation. <http://www.fda.gov/downloads/Drugs/.../Guidances/UCM174090.pdf>. (2009).
2. Andrade, R.J. *et al*. Drug-induced liver injury: an analysis of 461 incidences submitted to the Spanish registry over a 10-year period. *Gastroenterology* **129**, 512–521 (2005).
3. Björnsson, E. & Olsson, R. Outcome and prognostic markers in severe drug-induced liver disease. *Hepatology* **42**, 481–489 (2005).
4. Briz, O., Serrano, M.A., Maclas, R.I., Gonzalez-Gallego, J. & Marin, J.J. Role of organic anion-transporting polypeptides, OATP-A, OATP-C and OATP-8, in the human placenta-maternal liver tandem excretory pathway for foetal bilirubin. *Biochem. J.* **371**(Pt 3), 897–905 (2003).
5. Cui, Y., König, J., Leier, I., Buchholz, U. & Keppler, D. Hepatic uptake of bilirubin and its conjugates by the human organic anion transporter SLC21A6. *J. Biol. Chem.* **276**, 9626–9630 (2001).
6. Keppler, D. The roles of MRP2, MRP3, OATP1B1, and OATP1B3 in conjugated hyperbilirubinemia. *Drug Metab. Dispos.* **42**, 561–565 (2014).
7. Ritter, J.K. *et al*. A novel complex locus UGT1 encodes human bilirubin, phenol, and other UDP-glucuronosyltransferase isozymes with identical carboxyl termini. *J. Biol. Chem.* **267**, 3257–3261 (1992).
8. van de Steeg, E. *et al*. Complete OATP1B1 and OATP1B3 deficiency causes human Rotor syndrome by interrupting conjugated bilirubin reuptake into the liver. *J. Clin. Invest.* **122**, 519–528 (2012).
9. Kamisako, T. *et al*. Transport of monoglucuronosyl and bisglucuronosyl bilirubin by recombinant human and rat multidrug resistance protein 2. *Hepatology* **30**, 485–490 (1999).
10. Crawford, J.M., Ransil, B.J., Narciso, J.P. & Gollan, J.L. Hepatic microsomal bilirubin UDP-glucuronosyltransferase. The kinetics of bilirubin mono- and diglucuronide synthesis. *J. Biol. Chem.* **267**, 16943–16950 (1992).

11. Ehmer, U. *et al*. Gilbert syndrome redefined: a complex genetic haplotype influences the regulation of glucuronidation. *Hepatology* **55**, 1912–1921 (2012).

12. Erlinger, S., Arias, I.M. & Dhumeaux, D. Inherited disorders of bilirubin transport and conjugation: new insights into molecular mechanisms and consequences. *Gastroenterology* **146**, 1625–1638 (2014).

13. Fevery, J., Blanckaert, N., Heirwegh, K.P., Préaux, A.M. & Berthelot, P. Unconjugated bilirubin and an increased proportion of bilirubin monoconjugates in the bile of patients with Gilbert's syndrome and Crigler-Najjar disease. *J. Clin. Invest.* **60**, 970–979 (1977).

14. Levitt, D.G. & Levitt, M.D. Quantitative assessment of the multiple processes responsible for bilirubin homeostasis in health and disease. *Clin. Exp. Gastroenterol.* **7**, 307–328 (2014).

15. Chang, J.H., Plise, E., Cheong, J., Ho, Q. & Lin, M. Evaluating the in vitro inhibition of UGT1A1, OATP1B1, OATP1B3, MRP2, and BSEP in predicting drug-induced hyperbilirubinemia. *Mol. Pharm.* **10**, 3067–3075 (2013).

16. Campbell, S.D., de Morais, S.M. & Xu, J.J. Inhibition of human organic anion transporting polypeptide OATP 1B1 as a mechanism of drug-induced hyperbilirubinemia. *Chem. Biol. Interact.* **150**, 179–187 (2004).

17. Chiou, W.J., de Morais, S.M., Kikuchi, R., Voorman, R.L., Li, X. & Bow, D.A. In vitro OATP1B1 and OATP1B3 inhibition is associated with observations of benign clinical unconjugated hyperbilirubinemia. *Xenobiotica* **44**, 276–282 (2014).

18. Shoda, L.K., Woodhead, J.L., Siler, S.Q., Watkins, P.B. & Howell, B.A. Linking physiology to toxicity using DILIsym(®), a mechanistic mathematical model of drug-induced liver injury. *Biopharm. Drug Dispos.* **35**, 33–49 (2014).

19. Woodhead, J.L. *et al*. Application of a mechanistic model to evaluate putative mechanisms of tolvaptan drug-induced liver injury and identify patient susceptibility factors. *Toxicol. Sci.* **155**, 61–74 (2017).

20. Yang, K., Woodhead, J.L., Watkins, P.B., Howell, B.A. & Brouwer, K.L. Systems pharmacology modeling predicts delayed presentation and species differences in bile acid-mediated troglitazone hepatotoxicity. *Clin. Pharmacol. Ther.* **96**, 589–598 (2014).

21. Woodhead, J.L. *et al*. An analysis of N-acetylcysteine treatment for acetaminophen overdose using a systems model of drug-induced liver injury. *J. Pharmacol. Exp. Ther.* **342**, 529–540 (2012).

22. Ulloa, J.L. *et al*. Assessment of gadoxetate DCE-MRI as a biomarker of hepatobiliary transporter inhibition. *NMR Biomed.* **26**, 1258–1270 (2013).

23. Zucker, S.D. *et al*. Mechanism of indinavir-induced hyperbilirubinemia. *Proc. Natl. Acad. Sci. USA* **98**, 12671–12676 (2001).

24. Rotger, M. *et al*. Gilbert syndrome and the development of antiretroviral therapy-associated hyperbilirubinemia. *J. Infect. Dis.* **192**, 1381–1386 (2005).

25. Battista, C. *et al*. Mechanistic modeling with DILIsym® predicts species differences in CKA via multiple hepatotoxicity mechanisms. American Conference on Pharmacometrics 2016 (ACoP7). Abstract M-08. *J. Pharmacokinet. Pharmacodyn*. **43**(suppl. 1), 15 (2016).

26. Kuroda, M. *et al*. Increased hepatic and renal expressions of multidrug resistance-associated protein 3 in Eisai hyperbilirubinuria rats. *J. Gastroenterol. Hepatol.* **19**, 146–153 (2004).

27. Wolkoff, A.W. & Berk, P.D. 6. Bilirubin metabolism and jaundice. *Schiffs Diseases of the Liver*. 120–150 (John Wiley & Sons Ltd., 2012). <http://onlinelibrary.wiley.com/doi/10.1002/9781119950509.ch6/summary>.

28. Hsu, A. *et al*. Pharmacokinetic interaction between ritonavir and indinavir in healthy volunteers. *Antimicrob. Agents Chemother.* **42**, 2784–2791 (1998).

29. Smith, P.F. *et al*. Pharmacokinetics of nelfinavir and efavirenz in antiretroviral-naive, human immunodeficiency virus-infected subjects when administered alone or in combination with nucleoside analog reverse transcriptase inhibitors. *Antimicrob. Agents Chemother.* **49**, 3558–3561 (2005).

30. Kruse, G. *et al*. The steady-state pharmacokinetics of nelfinavir in combination with tenofovir in HIV-infected patients. *Antivir. Ther.* **10**, 349–355 (2005).

31. Chu, X. *et al*. Evaluation of cynomolgus monkeys for the identification of endogenous biomarkers for hepatic transporter inhibition and as a translatable model to predict pharmacokinetic interactions with statins in humans. *Drug Metab. Dispos.* **43**, 851–863 (2015).

32. Felsher, B.F. Effect of changes in dietary components on the serum bilirubin in Gilbert's syndrome. *Am. J. Clin. Nutr.* **29**, 705–709 (1976).

33. Griffin, P.M., Elliott, S.L. & Manton, K.J. Fasting increases serum bilirubin levels in clinically normal, healthy males but not females: a retrospective study from phase I clinical trial participants. *J. Clin. Pathol.* **67**, 529–534 (2014).

34. Li, R., Maurer, T.S., Sweeney, K. & Barton, H.A. Does the systemic plasma profile inform the liver profile? Analysis using a physiologically based pharmacokinetic model and individual compounds. *AAPS J.* **18**, 746–756 (2016).

35. Zucker, S.D., Goessling, W. & Hoppin, A.G. Unconjugated bilirubin exhibits spontaneous diffusion through model lipid bilayers and native hepatocyte membranes. *J. Biol. Chem.* **274**, 10852–10862 (1999).

36. McDonagh, A.F. Movement of bilirubin and bilirubin conjugates across the placenta. *Pediatrics* **119**, 1032–1033 (2007).

37. Fevery, J., Heirwegh, K. & De Groote, J. Renal bilirubin clearance in liver patients. *Clin. Chim. Acta* **17**, 63–71 (1967).

38. Fulop, M., Sandson, J. & Brazeau, P. Dialyzability, protein binding, and renal excretion of plasma conjugated bilirubin. *J. Clin. Invest.* **44**, 666–680 (1965).

39. Kotal, P. *et al*. Intestinal excretion of unconjugated bilirubin in man and rats with inherited unconjugated hyperbilirubinemia. *Pediatr. Res.* **42**, 195–200 (1997).

40. Schmid, R. & Hammaker, L. Metabolism and disposition of C14-bilirubin in congenital nonhemolytic jaundice. *J. Clin. Invest.* **42**, 1720–1734 (1963).

41. Jansen, P.L., Peters, W.H. & Lamers, W.H. Hereditary chronic conjugated hyperbilirubinemia in mutant rats caused by defective hepatic anion transport. *Hepatology* **5**, 573–579 (1985).

42. Muchova, L. *et al*. Bile acids decrease intracellular bilirubin levels in the cholestatic liver: implications for bile acid-mediated oxidative stress. *J. Cell. Mol. Med.* **15**, 1156–1165 (2011).

43. Muraca, M., Fevery, J. & Blanckaert, N. Relationships between serum bilirubins and production and conjugation of bilirubin. Studies in Gilbert's syndrome, Crigler-Najjar disease, hemolytic disorders, and rat models. *Gastroenterology* **92**, 309–317 (1987).

44. Nguyen, N. *et al*. Disruption of the UGT1 locus in mice resembles human Crigler-Najjar type I disease. *J. Biol. Chem.* **283**, 7901–7911 (2008).

45. Snell, A.M., Greene, C.H. & Rowntree, L.G. Diseases of the liver: II. A comparative study of certain tests for hepatic function in experimental obstructive jaundice. *Arch. Intern. Med.* **36**, 273–291 (1925).

46. Sathirakul, K. *et al*. Kinetic analysis of hepatobiliary transport of organic anions in Eisai hyperbilirubinemic mutant rats. *J. Pharmacol. Exp. Ther.* **265**, 1301–1312 (1993).

47. Stobie, P.E., Hansen, C.T., Hailey, J.R. & Levine, R.L. A difference in mortality between two strains of jaundiced rats. *Pediatrics* **87**, 88–93 (1991).

48. Zhou, J., Tracy, T.S. & Remmel, R.P. Bilirubin glucuronidation revisited: proper assay conditions to estimate enzyme kinetics with recombinant UGT1A1. *Drug Metab. Dispos.* **38**, 1907–1911 (2010).

49. Howell, B.A. *et al*. In vitro to in vivo extrapolation and species response comparisons for drug-induced liver injury (DILI) using DILIsym™: a mechanistic, mathematical model of DILI. *J. Pharmacokinet. Pharmacodyn.* **39**, 527–541 (2012).